Journal Pre-proofs

Prolonged endosperm filling and embryo enlargement phases contribute to the impaired development of inferior grains in *japonica* rice

Lu An, Yang Tao, Hao Chen, Ganghua Li, Yanfeng Ding, Matthew J. Paul, Zhenghui Liu

Please cite this article as: L. An, Y. Tao, H. Chen, G. Li, Y. Ding, M.J. Paul, Z. Liu, Prolonged endosperm filling and embryo enlargement phases contribute to the impaired development of inferior grains in *japonica* rice, *The Crop Journal* (2025), doi: https://doi.org/10.1016/j.cj.2025.06.004

This is a PDF file of an article that has undergone enhancements after acceptance, such as the addition of a cover page and metadata, and formatting for readability, but it is not yet the definitive version of record. This version will undergo additional copyediting, typesetting and review before it is published in its final form, but we are providing this version to give early visibility of the article. Please note that, during the production process, errors may be discovered which could affect the content, and all legal disclaimers that apply to the journal pertain.

Prolonged endosperm filling and embryo enlargement phases contribute to the impaired development of inferior grains in *japonica* rice

Lu An [a], Yang Tao [c], Hao Chen [a], Ganghua Li [a, b], Yanfeng Ding [a, b], Matthew J. Paul [d], Zhenghui Liu [a, b, *]

[a] College of Agriculture, Nanjing Agricultural University, Nanjing 211800, Jiangsu, China

[b] Collaborative Innovation Center for Modern Crop Production, Nanjing Agricultural University, Nanjing 211800, Jiangsu, China

[c] School of Breeding and Multiplication (Sanya Institute of Breeding and Multiplication), Hainan University, Sanya 572025, Hainan, China

[d] Sustainable Soils and Crops, Rothamsted Research, Harpenden, Hertfordshire AL5 2JQ, England, UK

Abstract: Inferior grains exhibit delayed developmental processes and reduced metabolic activities compared to superior grains, leading to unstable rice yield and quality. While significant advancements have been achieved in elucidating the physiology of endosperm filling in inferior grains, the role of the embryo remains underexplored and warrants comprehensive investigation. Two Wuyujing-3 mutants, DW024 (relatively synchronous; syn-DW024) and DW179 (significantly asynchronous; asyn-DW179), with different grain-filling patterns were used in this study. Samples of superior and inferior grains were collected at intervals from 5 to 60 d after fertilization and subsequently dissected into subsamples of the embryo and endosperm. Histochemical staining, biochemical analysis, and RNA sequencing (RNA-seq) were combined to systematically compare developmental and physiological traits between superior and inferior grains. Combining hierarchical clustering of mRNA datasets revealed three developmental phases of the endosperm and embryo: morphogenesis, endosperm filling/embryo enlargement, and maturation. In both syn-DW024 and asyn-DW179, the duration of the endosperm/embryo morphogenesis phase was identical in superior and inferior grains. The inferior grains of asyn-DW179 exhibited a 10-day prolongation in the endosperm filling phase and a 20-day extension in the embryo enlargement phase compared to the superior grains. The endosperm of inferior grains exhibited higher contents of sugars and free amino acids, along with slower accumulation of storage compounds, which was associated with the down-regulation of genes for starch synthesis and ABA signaling. In addition, transporters for nutrient exchanges between endosperm and embryo were down-regulated, suggesting a potential role of the embryo in adjusting the endosperm filling process. Collectively, our results reveal that the prolonged phases of endosperm filling and embryo enlargement may underlie the impaired development of inferior grains, offering a new perspective for breeding or cultivating rice with uniform grain quality.

Keywords: Rice; Inferior grain; Endosperm; Embryo; Grain development

1. Introduction

Rice panicles are composed of superior spikelets located on the primary branches and inferior spikelets positioned on the secondary branches. Compared to superior spikelets, inferior spikelets flower 3–4 d later and develop at a slower rate, leading to grains with reduced weight [1–4]. For instance, in the *japonica* rice cultivar Wuyunjing-24, inferior grains demonstrated a 45.8% decrease in the maximum filling rate and were 19.5% lighter in weight compared to superior grains [5]. Identifying the critical limiting factors contributing to the incomplete filling of inferior grains is essential for enhancing the uniformity of rice quality.

To date, the majority of related studies have primarily concentrated on the physiological differences between superior and inferior grains. These investigations encompass various aspects, including grain-filling dynamics,

carbon metabolism, hormonal regulation, and gene expression [1,5,6]. Results indicate that inferior grains undergo an extended period of developmental stagnation following fertilization, leading to a delayed initiation of grain filling [1,7]. Specifically, inferior grains display morphological stagnation as a result of an elongated syncytial phase during the early stages of grain filling and possess significantly fewer endosperm cell layers compared to superior grains at maturity. Metabolically, inferior grains display decreased enzymatic activities associated with carbohydrate metabolism, along with reduced expression levels of related genes [8,9]. Regarding hormonal regulation, abscisic acid (ABA) plays a pivotal role in modulating starch biosynthesis. Inferior grains exhibit markedly diminished ABA levels, and the application of exogenous ABA significantly boosts the enzymatic activities related to starch biosynthesis, thereby enhancing the filling performance of inferior grains [6,10,11]. However, the majority of studies have primarily concentrated on the physiological process of endosperm filling in superior and inferior grains, while overlooking developmental events in their embryos.

Rice grain comprises three genetically distinct tissues: the diploid embryo, the triploid endosperm, and the diploid maternal tissue, such as the pericarp. The endosperm serves as a nutrient source for the embryo, promoting its growth and facilitating germination. Successful embryo development is contingent upon proper endosperm formation; any failure in endosperm development will hinder embryo growth [12]. On the other hand, the embryo serves as the growth center and is prioritized for nutrient allocation, as it represents the next generation. It is reasonable to hypothesize that when nutrient availability is insufficient to support its development, the embryo may release specific signals to induce the remobilization of existing endosperm reserves [13]. Therefore, the development of both the embryo and endosperm must be tightly coordinated through physical and chemical interactions to ensure the formation of viable seeds. Recent molecular genetic studies have successfully identified the genes responsible for endosperm differentiation [14]. However, the interaction or communication between the endosperm and embryo remains largely unclear, and the significance of this process for grain filling warrants further investigation.

For rice, there is limited information available on the morphogenetic characteristics of inferior grains, especially with regard to the embryo and endosperm in comparison to superior grains. This study utilized an integrative analysis combining histochemistry, physiology, and transcriptomics to compare the developmental processes of both the endosperm and embryo in two Wuyujing-3 mutants, DW024 (relatively synchronous; syn-DW024) and DW179 (significantly asynchronous; asyn-DW179), which exhibit distinct grain-filling patterns. Our objective was to investigate the developmental and physiological processes of both superior and inferior grains, thereby elucidating the mechanisms underlying the incomplete filling of inferior grains. The results obtained are expected to offer novel insights into breeding high-quality rice by effectively narrowing the gap between inferior and superior grains.
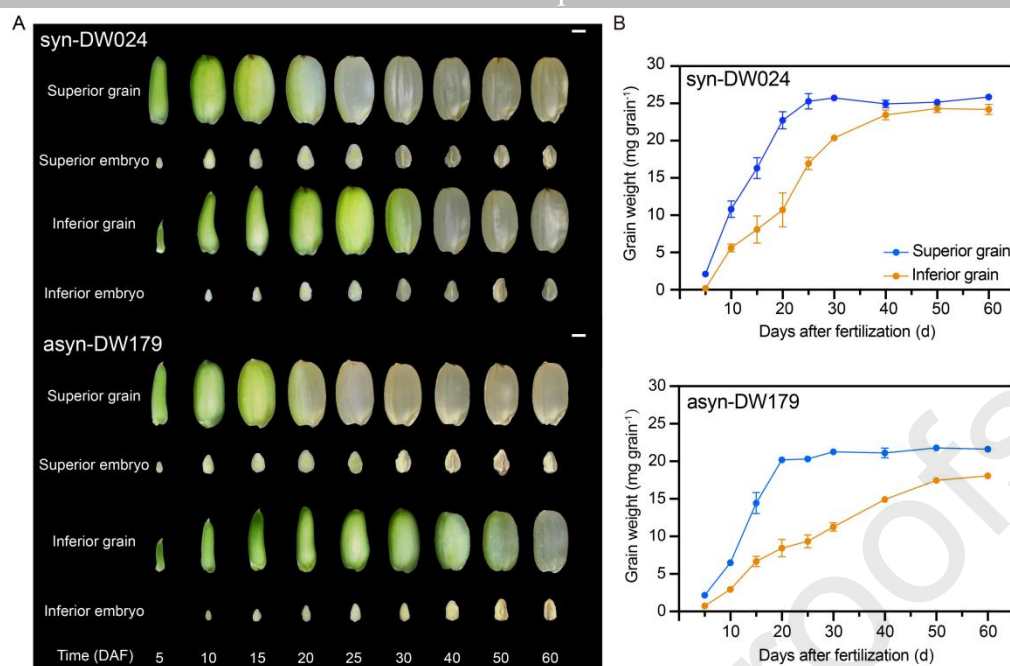
Fig. 1 – Time-series images of grains and embryos (A) and dynamics of grain weight (B) for superior and inferior grains.

DAF, days after fertilization. Scale bar, 1 mm.

2. Materials and methods

2.1. Plant materials and sampling

The mutants (syn-DW024 and asyn-DW179) used in this study were obtained by ethyl methane sulfonate (EMS) treatment of *japonica* cultivar Wuyujing-3 in 2007 [15]. After 15 years of continuous selection, the phenotypes of the two mutants have remained distinct and stable. The syn-DW024 exhibited relatively synchronous grain-filling characteristics, with a 10-day difference in the timing of maximum weight attainment between superior and inferior grains. In contrast, the asyn-DW179 displayed pronounced asynchrony, with a 20-day difference observed (Fig. 1). The two mutants were grown in field trials at the Danyang Experimental Station, China (31°54′31″N, 119°28′21″E) in 2021. The soil type of experiment was clay loam with pH 6.14, 17.76 g kg^{-1} organic matter, 1.02 g kg^{-1} total N, 0.61 g kg^{-1} total P, 11.62 g kg^{-1} total K, 29.26 mg kg^{-1} Olsen-P, and 127.07 mg kg^{-1} exchangeable K. The meteorological condition during rice growth season of 2021 were shown in Fig. S1.

The experimental plots, each measuring 3.5 m × 5.5 m, were arranged in a randomized complete block design with three replications. The 4-week-old seedlings were transplanted to the paddy field on June 18, 2021, at two seedlings per hill. The application rate of pure nitrogen was set at 270 kg ha^{-1}, while the application rates of phosphorus and potassium were 120 kg ha^{-1} (P_2O_5) and 192 kg ha^{-1} (K_2O), respectively. The fertilizers were applied in two equal doses, with one dose used for basal fertilization and the other for topdressing at the panicle initiation stage.

Flowering dates were recorded for the spikeletes on the middle primary rachis, and were labelled with plastic tags of varying colors. The spikelets/grains were sampled at nine time points: 5, 10, 15, 20, 25, 30, 40, 50, and 60 days after fertilization (DAF). The superior (on the top and middle primary branches) and inferior grains (on the bottom secondary branches) were separated and then immediately frozen in liquid nitrogen. All samples were stored

at −80 °C. Under the low-temperature conditions provided by a cryogenic box filled with dry ice, the samples were carefully dissected into embryos and endosperms. It should be noted that the collected endosperm samples included maternal tissues of pericarp and seed coat [16].

2.2. Gene expression profiling by RNA-seq

Total RNA extraction was performed using 0.1 g of the sample and TRIzol reagent (Invitrogen, Carlsbad, CA, USA). The RNA sample was solubilized in 100 μL of RNase-free water and subsequently quantified using a NanoDrop spectrophotometer (Thermo Scientific, Waltham, MA, USA). The quality of RNA was assessed by utilizing the Agilent 2100 Bioanalyzer (Agilent, Santa Clara, CA, USA). The sample library was subjected to quality checking and quantification using an Agilent 2100 Bioanalyzer and StepOnePlus Real-Time PCR System (Applied Biosystems, Waltham, MA, USA). The library products were sequenced using the BGISEQ-500 platform (BGI, Shenzhen, China). The RNA-seq libraries were analyzed by mapping the reads using the Nipponbare reference genome (IRGSP-1.0; https://www.ncbi.nlm.nih.gov/genome/?term=IRGSP-1.0).

To ensure high-quality and efficient mapping, we employed SOAPnuke (1.4.0) and Trimmomatic (0.36) to eliminate low-quality reads, retaining only clean reads for subsequent mapping using HISAT2 (2.1.0) [17–19]. The measurement of gene expression levels was performed using RSEM (1.2.8) [20], and the quantification of gene activity was based on fragments per kilobase of transcript per million mapped reads (FPKM) values. To eliminate the transcriptomic noise, genes exhibiting FPKM values ≥ 1 were considered as being expressed. In this study, the embryos and endosperms from superior and inferior grains were compared to obtain their $\log_2$ ratio at the same sampling time. The differentially expressed genes (DEGs) were considered statistically significant if their $\log_2$ ratio had an absolute value ≥ 1 and their false discovery rate (FDR)-corrected P-value was ≤ 0.001 [21].

2.3. Validation of transcriptome data using qRT-PCR

The quality of the RNA-seq data was confirmed by assessing the relative expression levels of five genes involved in starch and protein metabolism via qRT-PCR analysis (Fig. S2). Target-specific qRT-PCR primers were developed using the Primer 5.0 software [22] and subsequently synthesized, as detailed in Table S1. Each sample was represented by three biological replicates and three technical replicates. The comparison between qRT-PCR results and RNA-seq showed consistent expression patterns across both datasets, thereby confirming the reliability of the transcriptomic data.

2.4. Principal component analysis and hierarchical clustering

The principal component analysis (PCA) and hierarchical clustering (HCL) were performed using the OmicShare tools (https://www.omicshare.com/tools/Home/Soft). The standardized expression data were transformed into two dimensions, providing a clearer visual representation of the interrelationships among the 105 tissue samples for each mutant. Hierarchical clustering was conducted to classify the transcriptomic data in dendrograms.

2.5. Gene coexpression and functional enrichment analysis

The coexpression analysis was performed using MeV for genes in the endosperms and embryos of superior and inferior grains [23]. The relative expression levels for different tissues were calculated using the Z-score, and these calculated Z-scores were used as input for MeV. The individual datasets were clustered using the k-means method and Pearson correlation coefficients among genes. Functional categories were assigned to genes using Gene Ontology (GO) annotation [24]. The functional enrichment analysis was conducted in R using the phyper function with its default parameters [25]. P-value threshold was used as a criterion to identify GO categories that showed statistical significance (**, $P <0.01$).

4

2.6. Microscopic and histochemical observation

For the paraffin section, grain samples were fixed in a paraformaldehyde-glutaraldehyde fixation solution containing 2% paraformaldehyde (w/v) and 2.5% glutaraldehyde (v/v). The samples were dehydrated through an ethanol series, infiltrated with graded xylene-ethanol mixtures, and then underwent two pure xylene infiltrations. Xylene was replaced with pure paraffin, and then incubated for 3 days at 60 °C. The samples were embedded in paraffin, and sections (8 μm) were cut in the longitudinal plane for the embryo and the transverse plane for the endosperm. Sections were dewaxed with xylene, rehydrated through ethanol gradients, stained with 1% methyl violet, dehydrated in reverse ethanol gradients, and mounted for observation under a light microscope (BX53, Olympus, Japan).

2.7. Grain weight, size and germination rate measurement

Grain weight was measured by oven-drying the samples at 60 °C until they reached a constant weight. Grain length, width and thickness were measured using ImageJ software (version 1.53, National Institutes of Health, USA). Germination assays were performed on air-dried grains. For each time point, 50 grains with three biological replicates underwent surface sterilization with 1% H_2O_2 for 24 h, followed by rinsing with deionized water. Grains were germinated in petri dishes containing two layers of moist filter paper at 28 °C. The germination rate was calculated 14 days post-sowing, defined as radicle emergence > 1 mm.

2.8. Chemical analysis for metabolites

Sucrose, fructose, and glucose were quantified via ultra-high performance liquid chromatography (UHPLC Thermo UltiMate 3000, Waltham, MA, USA) following Chen et al. [26]. For 0.1 g samples, triplicate extractions using 80% (v/v) ethanol at 80 °C (30 min) were performed, and the mixtures were centrifuged (5000 r min^{-1}, 15 min). The pooled supernatants were analyzed by UHPLC, using a Shodex Asahipak (NH2P-50 4E column) coupled to an ELSD 6000 detector (Alltech, Deerfield, IL, USA). Post-extraction residues were quantified for starch content by digesting with 9.2 mol L^{-1} perchloric acid, reacting with anthrone reagent in boiling water (15 min), and then measuring spectrophotometrically at 620 nm.

Free amino acids were extracted from precisely weighed 0.1 g samples through sequential solvent processing: initially homogenizing in 1 mL of 80% (v/v) ethanol, followed by adding 3 mL of 4% (w/v) sulfosalicylic acid and then decomposing by ultrasonication for 20-min. After triple extraction cycles (5000×g, 25 min), the pooled supernatants were analyzed using a Hitachi L-8900 high-speed amino acid analyzer (Tokyo, Japan). The protein fractions (albumin, globulin, prolamin, and glutelin) of grains were extracted and measured by Ning et al. [27].

The extraction and purification of abscisic acid (ABA) were performed according to the optimized methodology of López-Cristoffanini et al. [28]. Three replicates of 100 mg of frozen samples were ground to a fine powder in liquid nitrogen. Then they were mixed with 1 mL of extraction medium (acetonitrile: H_2O: acetic acid, 90:9:1, v/v/v), extracted at 4 °C for 30 min, and centrifuged at 12,000 ×g for 10 min. The supernatants obtained from two extraction procedures were collected , evaporated and reconstituted in acetonitrile: H_2O (10:90, v/v) with 0.05% acetic acid. The samples were loaded onto Waters Sep-Pak C18 6cc cartridges. Cartridges were washed with 1 mL of 5% acetonitrile (0.05% acetic acid), and all fractions were collected. The solution was evaporated and reconstituted in 300 μL acetonitrile: H_2O (20:80, v/v, 0.05% acetic acid) and stored at −20 °C until analysis. ABA was quantified using SCIEX 6500 + Triple Quad LC-MS/MS System (AB SCIEX, Los Angeles, CA, USA).

2.9. Statistical analysis

The data of chemical analysis represent the mean values obtained from three independent measurements. Significant analysis was conducted using IBM SPSS Statistics (version 29.0, SPSS Inc., Chicago, IL, USA). The multiple

comparisons were assessed using Duncan's multiple range test (*, $P < 0.05$) in accordance with established academic conventions. GraphPad Prism (version 10.1.0, GraphPad Software, San Diego, CA, USA) was used for plotting.

3. Results

3.1. Endosperm and embryo development of superior and inferior grains

3.1.1. Endosperm development

Superior (SG) and inferior grains (IG) exhibit distinct cytohistological characteristics (Fig. 2). In SG, the parenchyma cells filled the cavity of endosperm sac by 5 DAF, with most of the cells having completed cellularization. At 10 DAF, the endosperm had differentiated into starchy endosperm and aleurone layers and had begun to accumulate storage reserves such as starch and protein. In IG, endosperm cellularization initiated at 5 DAF; the central region was occupied by the vacuole, and the peripheric cells began to form cell walls. The cellularization of IG endosperm was completed by 10 DAF, and then differentiated into starchy endosperm and aleurone layer. Morphologically, IG endosperm had a similar pattern of development to SG endosperm, but it had a smaller size.

Compared with syn-DW024, the delayed development of endosperm in IG of asyn-DW179 was mainly manifested in the volume expansion of endosperm. Generally, for both materials, the grain length of superior grains reached its maximum at 10 DAF, while grain width and thickness peaked at 20 DAF. In syn-DW024, the inferior grains showed a parallel lag in all three dimensions. By contrast, in asyn-DW179, the difference between SG and IG in asyn-DW179 was more pronounced after 10 DAF (Fig. S3). For example, the grain length of IG in syn-DW024 reached its maximum at 10 DAF, 5 d later than that of SG. However, in asyn-DW179, that was 20 days later than that of SG.
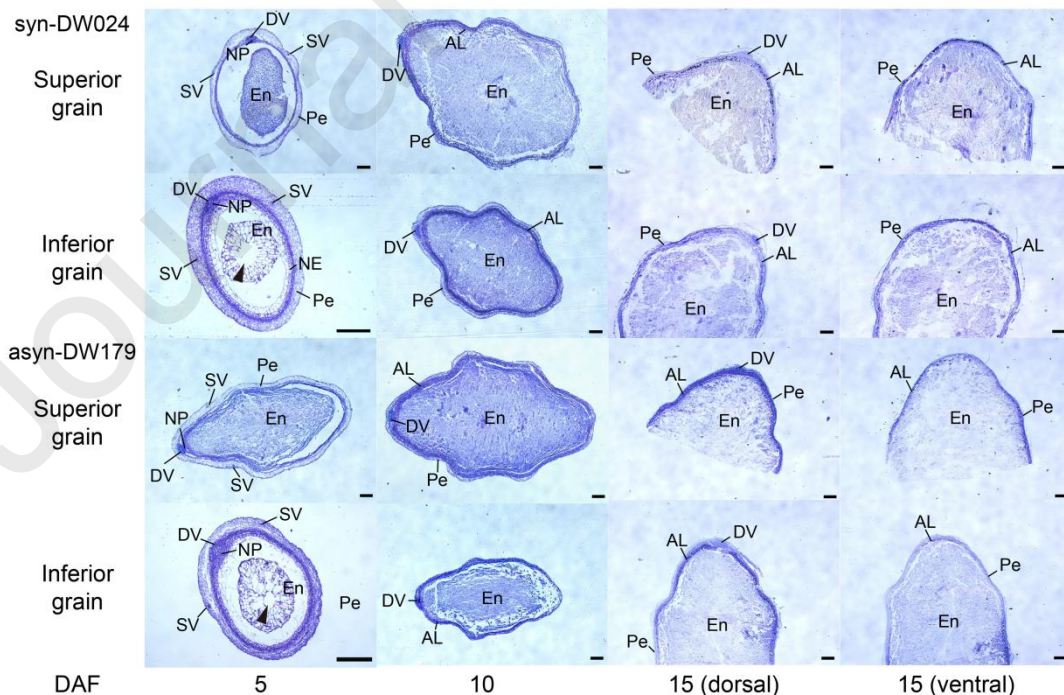

Fig. 2 – Histological pictures for the endosperm of superior and inferior grains during developmental processes.

At 5 DAF, cavities (arrowhead) are observed in the endosperm sac of inferior grains, suggesting that the process of cellularization

remains incomplete. In contrast, superior grains have completed endosperm cellularization. AL, aleurone layer; DAF, days after fertilization; DV, dorsal vascular bundle; En, endosperm; NE, nucellar epidermis; NP, nucellar projection; Pe, pericarp; SV, lateral stylar vascular trace. Scale bar, 200 μm.

3.1.2. Embryo development

The process of embryo morphogenesis was compared between the SG and IG collected from 5 to 20 DAF (Fig. 3A). The embryo of SG initiated formation of shoot apical meristem at 5 DAF and completed the majority of its developmental events by 10 DAF, giving rise to the tissues of the coleoptile, plumule, and radicle. From 10 to 20 DAF, the SG embryo transitioned into the enlargement phase.

On the other hand, IG exhibited severe retardation in embryo morphogenesis, in particular asyn-DW179 (Fig. 3A). At 5 DAF, the protrusion of the coleoptile on the ventral side was visible in IG of syn-DW024, indicating the initiation of embryo morphogenesis. Meanwhile, the embryo in asyn-DW179 was still at the globular phase, with no apparent morphological differentiation. Like the SG, IG completed the embryo morphogenesis at 10 DAF but with smaller volume compared to SG. After 10 DAF, the IG showed a marked delay in the process of embryo enlargement.

The germination rate is an indicator of the physiological maturity of the embryo. Part of the superior grains had the capability to germinate at 10 DAF. At 20 DAF, the SG reached the maximum germination rate, indicating the completion of morphogenesis and the initiation of dormancy (Fig. 3B). However, the germination rates of the IG peaked at 40 DAF, being 20 days later than those of SG. In syn-DW024, the germination rate of IG was over 60% by 20 DAF, while it was still below 40% until 30 DAF in asyn-DW179.
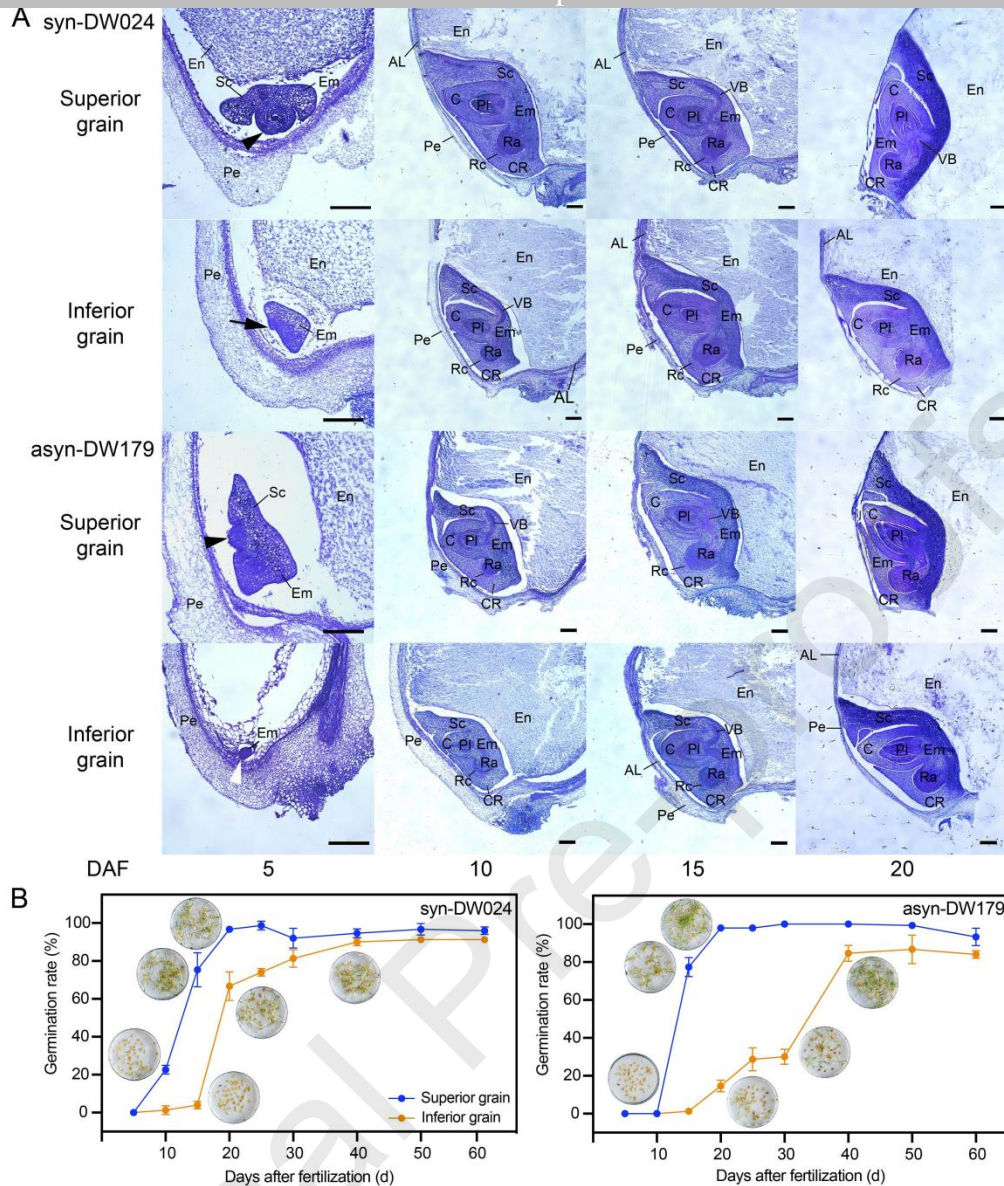
Fig. 3 – Histological pictures for the embryo of superior and inferior grains during developmental processes.

(A) Longitudinal sections of developmental embryos. At 5 DAF, the embryo of the superior grains differentiates into the shoot apics meristem (black arrowhead). The coleoptile primordium (black arrow) is visible in the inferior grains of syn-DW024, while the globular embryo (white arrowhead) can be recognized in asyn-DW179. After that, the embryos of superior and inferior grains are morphologically similar, with some differences in volume. (B) Germination rates of grains at different developmental timepoints of the embryo. AL, aleurone layer; C, coleoptile; CR, coleorrhiza; DAF, days after fertilization; Em, embryo; En, endosperm; Pe, pericarp; Pl, plumule; Ra, radicle; Rc, root cap; Sc, scutellum; VB, vascular bundle. Scale bar, 200 μm. Each value in (B) represents the mean ± SE of three replicates.

3.2. Developmental phases and transcriptional pattern of the superior and inferior grains

Gene expression differences were detected between SG and IG by comparing transcriptomes of the endosperms and embryos (Fig. 4A). Most genes were expressed at the early and middle phases of grain development. The IG exhibited a higher number of expressed genes compared to SG, and the embryo displayed a greater number of expressed genes than the endosperm. To validate the purity of the different tissues, the transcriptomic data were analyzed using dimensionality reduction with PCA (Fig. 4B). The first principal component (PC1) effectively separated the embryo from the endosperm, explaining 38.0% and 41.3% of the variance respectively. Meanwhile,

8

PC2 successfully distinguished between different developmental phases in both materials, accounting for 21.1% and 20.3% of the variance.

Hierarchical cluster analysis of the transcriptome showed the divergent developmental patterns between SG and IG. As demonstrated in the dendrograms, three clusters were identified for both the endosperms and embryos of SG and IG (Fig. 4C). Accordingly, we divided the whole development phase of rice grain into three phases, and described the transcriptional pattern for each phase using gene coexpression (Figs. S4 and S5) and functional enrichment analysis (Figs. S6 and S7).

The three developmental phases of the endosperm shared a common pattern for both SG and IG (Fig. 4C). (i) Phase I, 0–5 DAF, was defined as the morphogenesis phase. GO enrichment analysis revealed that this phase was characterized by genes associated with cell division, cell cycle, DNA replication, transcription, translation, cell wall biosynthesis, and starch synthesis (Figs. S6 and S7). (ii) Phase II, from 10 to 20 DAF (for SG) or to 30 DAF (for IG), was designated as the endosperm filling phase. This phase featured genes responsible for organ growth, starch biosynthesis, and amino acid transport. (iii) Phase III, the maturation phase, was significantly enriched in GO terms associated with iron ion binding, responses to biotic and abiotic stresses, hormonal responses, and defense mechanisms (Figs. S6 and S7).

Interestingly, the SG and IG were similar in the time lapse of Phase I but contrastingly different in that of Phase II. This is especially obvious for the IG (Fig. 4C). In syn-DW024, the IG had the same duration of Phase II as the SG. However, in asyn-DW179, Phase II lasted until 30 DAF, a ten-day delay compared to the SG. Consequently, the onset of the maturation phase was delayed until 40 DAF.

Similarly, for the embryo, the three developmental phases showed a shared pattern in both SG and IG (Fig. 4D). (i) Phase I, 0–5 DAF, was referred to as the morphogenesis phase. It included an overabundance of GO terms such as cell cycle, cell differentiation, and cell wall modification (Figs. S6 and S7). (ii) Phase II, from 10 to 20 DAF (for SG) or to 40 DAF (for IG), was referred to as the embryo enlargement and desiccation phase. GO enrichment terms of this phase were mainly associated with starch biosynthesis, amino acid transport, seed dormancy process, and defense response (Figs. S6 and S7). (iii) Phase III, the maturation and dormancy phase, was enriched in GO terms characteristic of metal ion binding, response to biotic and abiotic stresses, hormone response, and defense response (Figs. S6 and S7).

The time lapse of Phase I was similar in both SG and IG embryos for both materials (Fig. 4D). However, notable variations were observed in Phase II between synchronous and asynchronous materials. Syn-DW024 had the same Phase II for both SG and IG, lasting from 10 DAF to 30 DAF. By contrast, asyn-DW179 had a longer Phase II (from 10 to 40 DAF) in IG, extending by 20 days compared to SG.
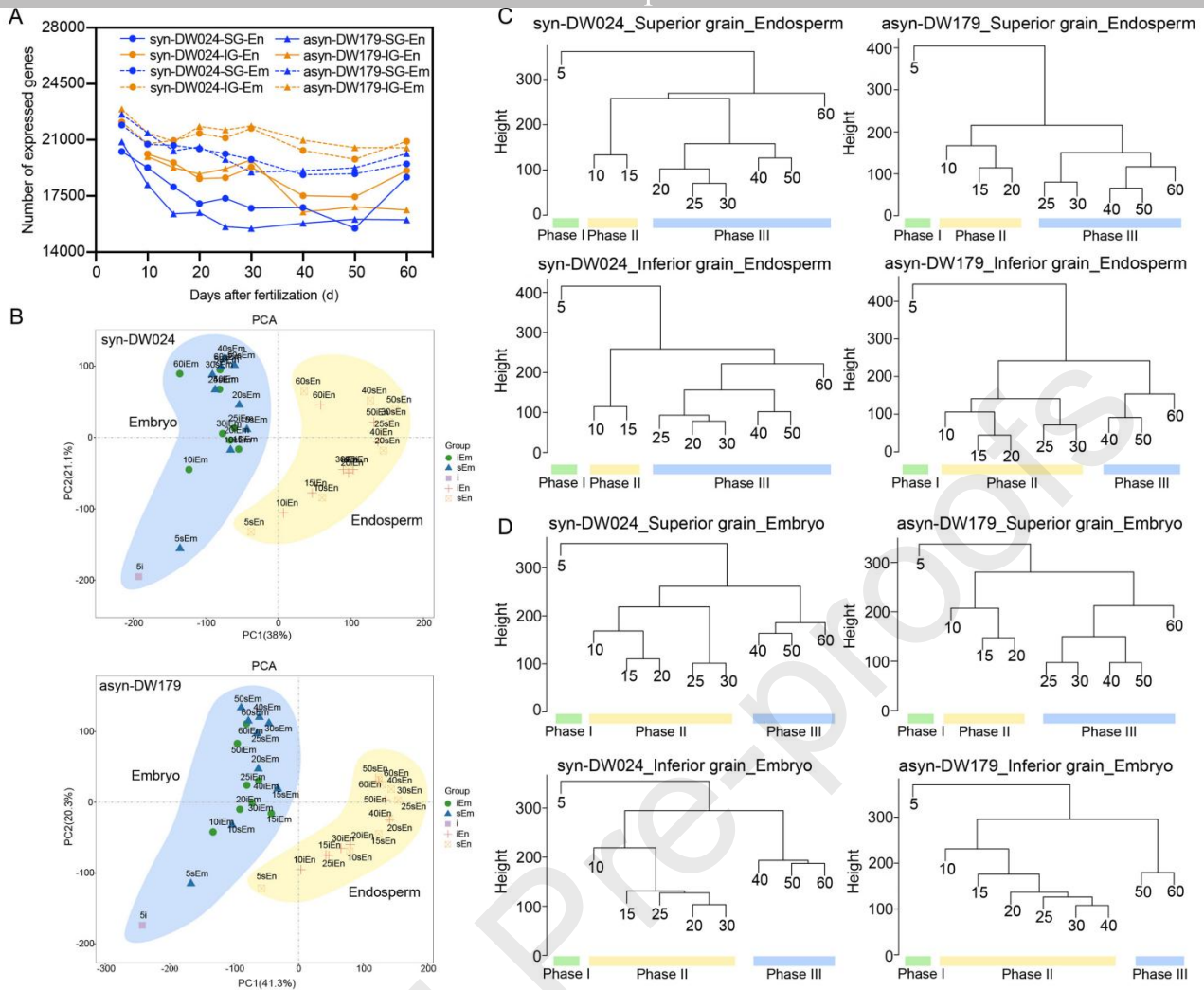
Fig. 4 – Global-scale transcriptome relationships across tissues and developmental phases.

(A) Number of genes detected in each tissue of superior and inferior grains. (B) PCA of mRNA populations from various tissues, showing the mRNA populations from superior and inferior grain can be divided into two distinct groups, the embryo and the endosperm. Note that the inferior grain sample at 5 DAF contains embryo, thus falling into the group of embryos. (C) The clustered dendrogram depicting the global transcriptome relationships of time series samples from the endosperm of superior and inferior grain. (D) The clustered dendrogram depicting the global transcriptome relationships of time series samples from the embryo of superior and inferior grain. The numbers 5, 10, 15 ..., and 60 represent the days after fertilization.

3.3. Metabolic dynamics of endosperms and embryos in superior and inferior grains

3.3.1. Sugars

The sucrose content in both the embryo and endosperm decreased gradually during grain development, and the fructose and glucose contents exhibited a similar trend (Figs. 5A and A'; S8A and B). In the early phase of grain development, the endosperm and embryo of IG exhibited significantly higher soluble sugar content compared to those of SG. As starch accumulation neared completion, the soluble sugar content in both IG and SG remained relatively stable, with no noticeable fluctuations.

Compared with syn-DW024, the soluble sugar content of endosperm and embryo in asyn-DW179 decreased more slowly (Figs. 5A'; S8A and B). In the endosperm, sucrose and fructose decreased to the lowest value at 40 DAF, and glucose decreased at 30 DAF in IG of syn-DW024, which was 20 or 10 days later than in SG. However, for the

asyn-DW179, the three soluble sugars exhibited a 25-day lag in IG. In the embryo, sucrose decreased to the lowest value at the same time for both SG and IG in syn-DW024. For the asyn-DW179, there was a 10-day lag in the IG. Fructose and glucose of IG in syn-DW024 exhibited a delay of 10 days and 20 days, respectively. In contrast, asyn-DW179 demonstrated a uniform 25-day delay for both types of soluble sugars.

Invertase (INV) and sucrose synthase (SuS) catalyze the breakdown of sucrose. Most of the SuS and INV genes in the endosperm were expressed during the period of rapid sucrose decline, and their expression was significantly prolonged in IG (Fig. 5A and A'). In the embryo, the expression of these enzyme genes primarily occurred during early development and the maturation phase, and their expression levels were markedly delayed in IG.

3.3.2. Starch

The starch content in the endosperm progressively increased during grain development, whereas it remained relatively stable in the embryo. The endosperm demonstrated significantly higher starch content compared to the embryo (Fig. 5B and B'). The starch content in the endosperm of IG was lower than that of SG during grain development, while that of the embryo in IG was slightly higher or not much different from that of SG.

For both syn-DW024 and asyn-DW179, the starch content of endosperm reached the maximum level at 40 DAF in IG, 15 days later than that of SG (Fig. 5B and B'). In syn-DW024, the starch content in IG was 7.25% lower than that in SG, whereas in asyn-DW179, the starch content in IG was 11.06% lower than that in SG. In syn-DW024, the starch content in the embryo of IG was always slightly higher than that in SG. However, in asyn-DW179, the starch content in SG and IG was not significantly different before 50 DAF. After 50 DAF, the starch content of the embryo in IG was higher than that in SG.

There were differences in the expression patterns of starch synthesis genes in endosperm and embryo, such as ADP-glucose pyrophosphorylase, starch branching enzyme and starch synthase (Fig. 5B and B'). The initiation of gene expression in IG was significantly delayed by 5 days and extended to 40 DAF compared with SG. In embryo, genes for starch synthesis were expressed during its development, and a delayed initiation of α-amylase genes expression involved in starch degradation was also observed in IG.

3.3.3. Storage proteins

Storage protein content in the endosperm increased progressively during grain development, while free amino acids (FAAs) levels gradually decreased and stabilized (Figs. 5C and C'; S8C). The storage protein content in IG was lower than that in SG, but the FAA content in IG was higher than that in SG before 40 DAF. In syn-DW024, the storage protein content reached maximum at 25 DAF in IG, and 5 days later than that in SG. In asyn-DW179, it reached maximum at 60 DAF in IG, and 35 days later than that in SG. The protein components exhibited a consistent trend with the total protein content (Fig. S9). In both materials, the FAA content reached a minimum at 40 DAF in IG, which was 20 days later than that in SG.

The genes for glutelin and prolamin synthesis were predominantly expressed in the endosperm, while the globulin genes exhibited specific expression in the embryo (Fig. 5C and C'). In the endosperm, Syn-DW024 exhibited a 5-day delay in the initiation of IG gene expression compared to SG, whereas asyn-DW179 demonstrated significantly greater latency, exceeding 10 days. In the embryo, the globulin gene (*OsEnS-115*) was expressed for an extended duration of 5 days in syn-dw024, whereas its expression was prolonged by 20 days in asyn-DW179.

3.4. ABA contents of endosperms and embryos in superior and inferior grains

The ABA content exhibited an inverted 'V'-shaped distribution in the endosperm, while in embryo it increased

gradually with the development and maturation of the grain (Fig. 5D and D'). In the endosperm, ABA levels peaked at 15 DAF in SG, but they reached a maximum at 20 DAF in IG. Post-peak levels of ABA in IG were higher than those in SG. In embryos, the ABA content in SG increased steadily from 10 to 30 DAF. In contrast, in IG, the ABA content initially decreased slightly and then increased, remaining consistently lower than that in SG until maturation.

In the endosperm of syn-DW024 and asyn-DW179, ABA content peaked at 15 DAF in SG compared to 20 DAF in IG, with post-peak levels in IG surpassing those in SG (Fig. 5D and D'). Specifically, the peak value in the IG of syn-DW024 was reduced by 7.24% relative to SG, while the IG of asyn-DW179 exhibited a more pronounced decrease of 27.22%.

In the endosperm, genes responsible for ABA synthesis were expressed from 5 to 20 DAF in SG, and from 5 to 40 DAF in IG. The ABA-deactivating genes were expressed mainly in the endosperm and also showed prolonged or delayed expression in IG (Fig. 5D and D'). Most genes for ABA synthesis in embryos were expressed in the maturation phase. In contrast to syn-DW024, the expression activation delay of these genes in the IG of asyn-DW179 was more pronounced, with a delay of approximately 25 days compared to that in SG.
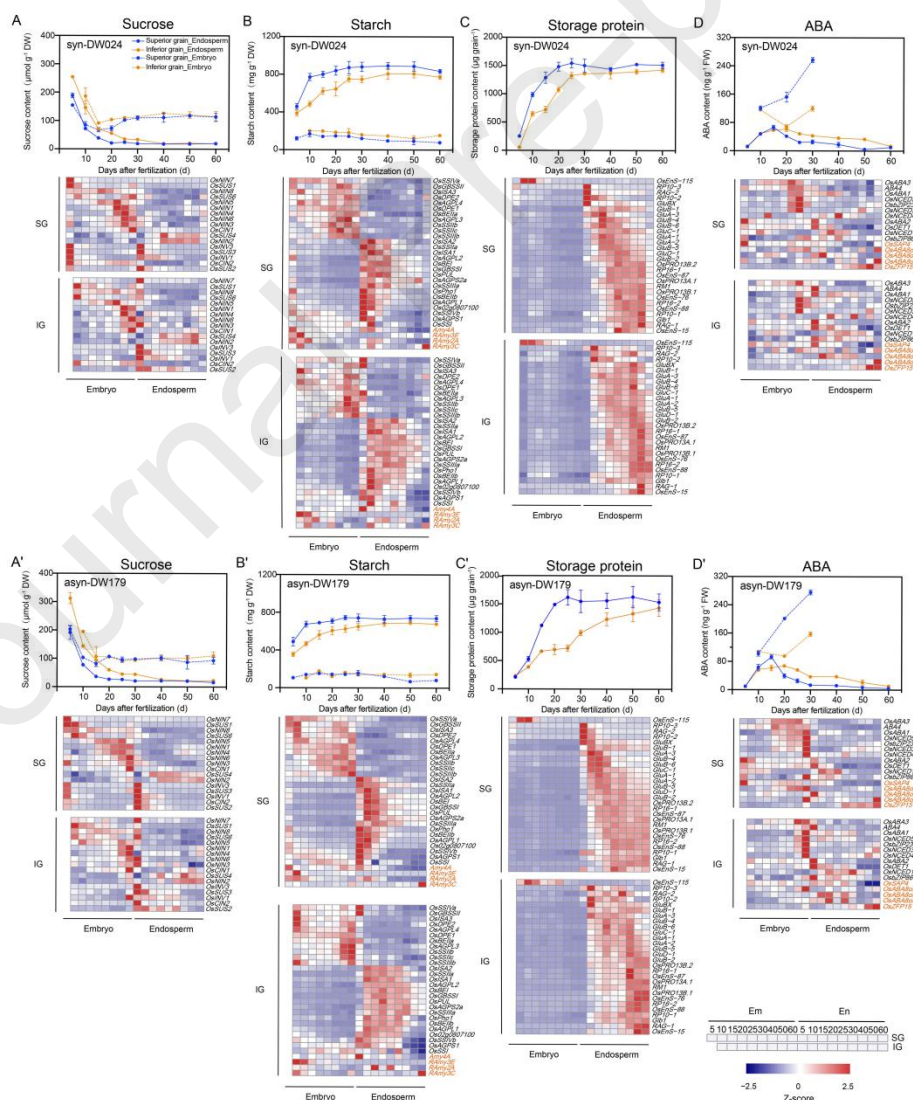

Fig. 5 – Sucrose, starch, storage protein, ABA and their regulating genes in the endosperm and embryo of syn-DW024 (A–D)

12

and asyn-DW179 (A–D').

Genes related to starch or ABA metabolism are marked in orange. Each value represents the mean ± SE of three replicates. The FPKM value for each gene is presented after normalization with the maximum value across all time points.

4. Discussion

In this study, morphological, physiological, and molecular comparative analyses were conducted on the endosperms and embryos of superior and inferior grains in two mutants exhibiting synchronous and asynchronous grain-filling patterns. Accordingly, we present a comprehensive and dynamic overview of rice seed development (Fig. 6), revealing that the prolonged enlargement of the embryo, delayed endosperm filling, and the resultant insufficient synthetic capacity of storage reserves are likely the primary factors contributing to the impaired development of inferior grains.
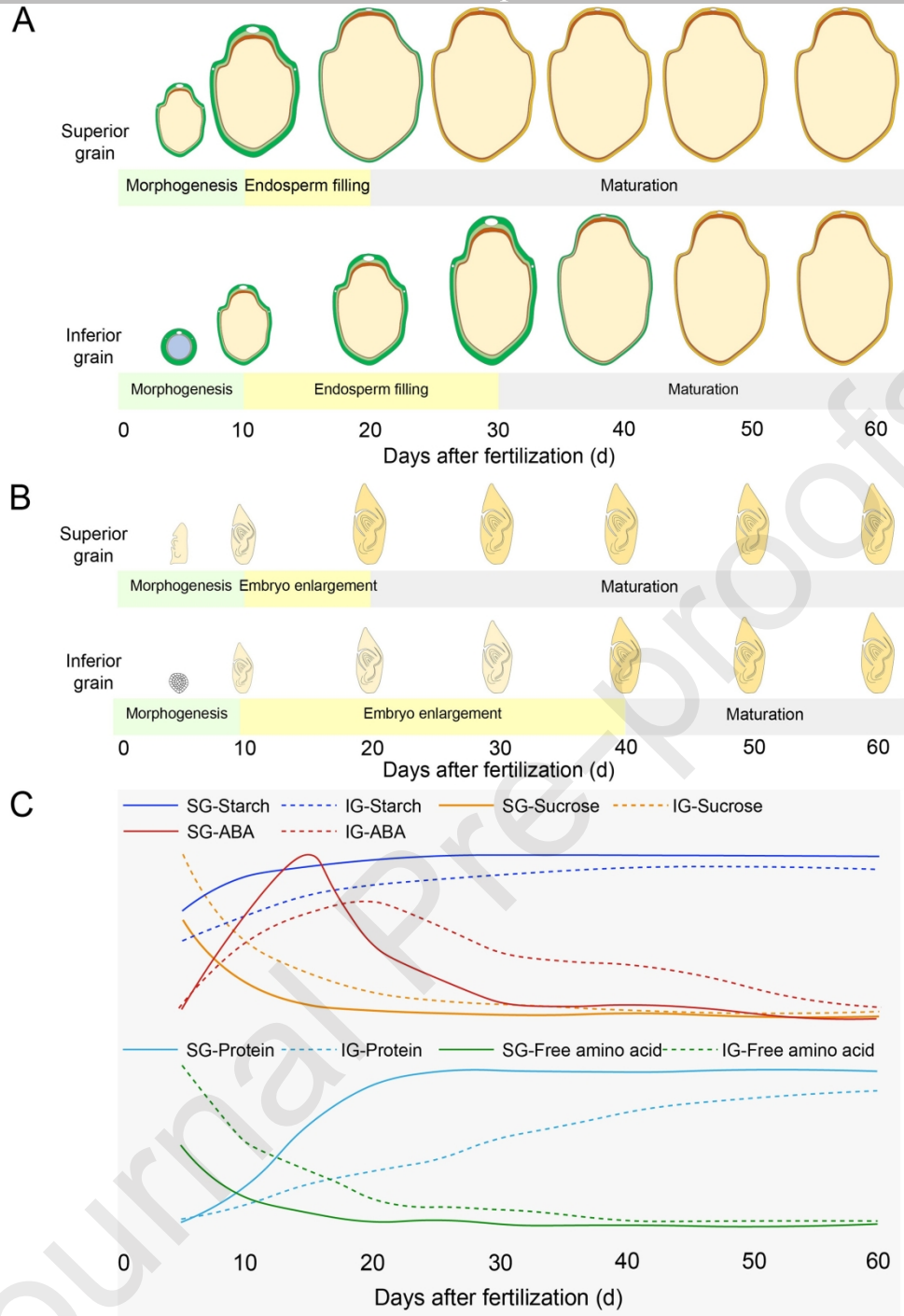
Fig. 6 – Classification of developmental phases of the superior and inferior grains, along with their morphological characteristics and reserve accumulation dynamics.

(A) Morphological changes of the endosperm (transverse section). (B) Morphological changes of the embryo (longitudinal section). (C) Dynamic accumulation of storage materials (sucrose, starch, free amino acid, storage proteins) and ABA in the endosperm.

4.1. The delayed endosperm filling in the inferior grains and its physiological mechanism

In general, a rice grain consists of 2–3% embryo and 89–94% starchy endosperm, and the remainder comprising maternal tissues and the aleurone layer [29]. The endosperm constitutes the largest portion of the whole grain and therefore plays a dominant role in determining its physicochemical and physiological properties. Weak

physiological activity in the endosperm has long been regarded as a primary factor contributing to the delayed development of inferior grains. So far, studies investigating the slow initiation of grain filling in inferior grains have predominantly emphasized the source-sink relationship, storage accumulation, phytohormone signaling, and gene expression regulation [6, 8, 30, 31]. However, limited research has been conducted on the developmental aspects of the inferior endosperm, particularly regarding the morphogenetic processes in comparison to those of the superior grains.

Based on the transcriptional patterns of superior and inferior grains in synchronous and asynchronous materials, we further subdivide rice endosperm development into three consecutive phases: the morphogenesis phase, the endosperm filling phase, and the maturation phase. A more detailed analysis of the developmental characteristics reveals that inferior grains experience a prolonged duration during the second phase, specifically the endosperm filling phase. Notably, it is not the first phase, the morphogenesis phase, but rather the filling phase, that differentiates inferior grains from superior grains. This contrasts with previous findings, which indicate that the timing of endosperm cell division and cellularization in inferior grains occurs later than in superior grains. For example, Ishimaru et al. [1] reported that inferior grains displayed morphological stagnation during the very early stage of grain filling. Subsequently, when grains started to elongate, the endosperm's morphological development in both superior and inferior grains became indistinguishable. On the other hand, we observed that inferior grains exhibited similar cellular activities during the morphogenesis phase as superior grains, including cell division, DNA replication, transcription, translation, cell wall biosynthesis, and starch synthesis. Additionally, the endosperm filling phase of inferior grains was significantly prolonged, lasting approximately 10 days longer (Fig. 4C). Therefore, in addition to the morphogenetic phase, the endosperm filling phase may also play a critical role in the development of inferior grains.

Our results show that the delayed endosperm filling may be the main reason for the weakness of the inferior grains. However, the underlying mechanism is still open. Endosperm filling is mainly characterized by the accumulation of starch and protein. Photosynthetic assimilate limitation was traditionally considered the main cause of poor development of inferior grains [32]. However, recent studies indicate that carbohydrate supply is not the primary issue since adequate sucrose is available at the start of grain filling [33]. Instead, evidence suggests that low activities of key enzymes in carbon metabolism may be responsible for the poor grainfilling [34]. In this study, we observed that inferior grains exhibited higher levels of soluble carbohydrates and free amino acids, along with weaker expression of starch and protein biosynthetic genes. These findings reinforce our previous conclusion that assimilate limitation is not the primary factor influencing grain filling in inferior grains [35], highlighting a potential bottleneck for the onset of endosperm filling.

The phytohormones, such as auxin, cytokinin, and abscisic acid, serve as crucial endogenous signaling molecules in plants and play essential roles in key processes, including cell division, differentiation, and maturation during grain development and filling [36, 37]. Among them, ABA plays a crucial role in modulating the activity of key enzymes during grain filling, especially those involved in starch biosynthesis, as the peak ABA content coincides with the onset of starch accumulation [38]. Lower ABA content was associated with the insufficient filling of inferior grains [6, 39]. To elucidate the molecular network by which ABA regulates endosperm filling, we performed a comprehensive analysis of the expression patterns of genes involved in starch synthesis (Figs. S10 and S11). In superior grains, five starch biosynthesis-related transcription factors (*RPBF*, *OsbZIP58*, *NF-YC12*, *NF-YB1*, and *bHLH144*) exhibited high expression levels from 5 DAF to 15 DAF. This temporal expression pattern closely corresponded to the dynamic increase in ABA content observed in superior grains (Fig. 5D and D'). Simultaneously, five genes involved in starch synthesis (*OsAGPL3*, *OsGBSSI*, *OsBEIIb*, *OsISA1*, and *OsAGPL2*) displayed a similar expression trend. In contrast, IG showed a pronounced temporal delay in gene expression within the endosperm. The expression of these transcription factors began approximately 5 days later than in SG, with most achieving peak

expression levels between 10 and 25 DAF. This delayed expression pattern closely mirrored the trend of ABA accumulation in IG. Collectively, our results suggest that the ABA-signaling network may play a pivotal role in initiating endosperm filling in inferior grains.

4.2. The retarded embryo enlargement in the inferior grains and its potential influence on endosperm filling

The embryo, despite its small size, significantly influences endosperm development. Nutrients from maternal tissues are initially stored in the endosperm, then either used to synthesize storage compounds such as starch and proteins or transferred to the developing embryo. Thus, the endosperm controls nutrient allocation within the seed. However, the embryo is central to seed development, and the endosperm's role is widely seen as altruistic, sacrificing itself to nourish the embryo [40, 41]. It is thus speculated that the embryo exerts a counter-regulatory force on the endosperm, supported by growing evidence. Previously, we applied a novel comparison method based on a notched-belly mutant, DY1102, and demonstrated a direct effect of the embryo on the developmental processes of the endosperm [16]. The integrated analysis of the transcriptome and metabolome revealed putative regulatory mechanisms that coordinate the developmental processes between the embryo and endosperm. External signals for endosperm regulation may include hormones such as GA secreted by the embryo, whereas the internal regulatory mechanism could involve the T6P–SnRK1 signaling pathway, which mediates carbon allocation within the endosperm.

This study revealed a high degree of synergy in the morphogenetic processes of both the embryo and endosperm in superior grains. In these grains, both the embryo and endosperm initiated morphogenesis at 5 DAF and completed their development by approximately 20 DAF. In inferior grains, although embryo morphogenesis completes by 10 DAF, subsequent enlargement and maturation are significantly delayed, with embryo maturation occurring about 20 days later than in superior grains, as indicated by the germination rate. During the maturation phase, dormancy induction is dependent on ABA signaling, which is primarily regulated by the balance between ABA biosynthesis and degradation [42]. In this study, the ABA content in the embryos of superior grains increased rapidly following morphogenesis, whereas in inferior grains, the ABA content showed minimal change until 20 DAF, leading to a 10-day delay in embryo maturation. Collectively, we speculate that delayed embryo development in inferior grains may contribute to the prolonged endosperm filling period.

Results from Arabidopsis and rice show that the embryo and endosperm become symplastically isolated soon after fertilization, requiring communication across the apoplast [43]. The apoplastic interfaces between compartments and the adjacent cells are critical for understanding nutrient and signal exchanges. Nutrient flow across the apoplast depends on transporters at these interfaces, and transporter dysfunction can disrupt nutrient flow, leading to arrested embryo development [13]. In this study, we observed a highly coordinated expression pattern of transporter genes in both the embryo and endosperm during the grain-filling phase, including those involved in the transport of sucrose, amino acids, lipids, and mineral nutrients (Fig. S12). Among them, sucrose and hexose transporters (OsSWEET14) as well as amino acid transporters (OsUMAMIT9) displayed distinct expression patterns specifically in the embryo-surrounding endosperm, consistent with the findings reported by Tao et al. [16]. In contrast, the transporters in inferior grains either initiated expression with a delay or maintained expression for an extended duration. So far, the mechanism of action of transporters as signals for the communication between the embryo and the endosperm is not perfectly understood. In addition, the proposed genes or pathways associated with the retarded development of inferior grains require verification through in-depth molecular experiments.

5. Conclusions

Using two representative materials, we compared the developmental processes of the endosperm and embryo between superior and inferior grains to explore the mechanisms underlying the delayed development of inferior

grains. An integrated analysis of transcriptome data and histochemical characteristics revealed distinct morphogenetic patterns of embryos and endosperms in the two types of grains. Notably, while the initial morphogenesis phases of endosperm and embryo were similar between superior and inferior grains, the inferior grains exhibited significant delays in their developmental progression, particularly in the prolonged endosperm filling phase and extended embryo enlargement phase. The extended duration of endosperm filling in inferior grains was accompanied by reduced expression of genes involved in starch and storage protein biosynthesis, despite the higher levels of their substrates, the free sugars and amino acids. This phenomenon might be linked to the low content of ABA, which plays a promoting role in starch accumulation. Furthermore, the downregulation of transporters suggests a potential regulatory role of the embryo in endosperm development. Our findings provide new insights into the developmental and physiological mechanisms underlying inferior grain formation, thereby offering innovative strategies for improving rice grain yield and quality through genetic or agronomic approaches.

Data availability statement

All the analyzed data relevant to this manuscript are present in this paper and its supplementary data. All the raw data associated with this study have been submitted to NCBI and are available under accession number PRJNA1253084 (https://www.ncbi.nlm.nih.gov/sra/) and ScienceDB (https://www.scidb.cn/c/CJ).

Declaration of competing interest

The authors declare that they have no known competing financial interests or personal relationships that could have appeared to influence the work reported in this paper.

CRediT authorship contribution statement

Lu An: Investigation, Data curation, Formal analysis, Validation, Visualization, Writing - original draft, Writing - review & editing. **Yang Tao**: Writing - original draft, Funding acquisition. **Hao Chen**: Methodology, Investigation. **Ganghua Li**: Writing - review & editing, Supervision, Project administration. **Yanfeng Ding**: Writing - review & editing, Supervision, Project administration. **Matthew J. Paul**: Writing - review & editing. **Zhenghui Liu**: Conceptualization, Supervision, Project administration, Methodology, Writing - original draft, Writing - review & editing, Funding acquisition.

Acknowledgments

Appendix A. Supplementary data

Supplementary data for this article can be found online at http://doi.org/10.1016/j.cj.2025.xx.xxx.

References

[1] T. Ishimaru, T. Matsuda, R. Ohsugi, T. Yamagishi, Morphological development of rice caryopses located at the different positions in a panicle from early to middle stage of grain filling, Funct. Plant Biol. 30 (2003) 1139−1149.

[2] P. Mohapatra, R. Patel, S. Sahu, Time of flowering affects grain quality and spikelet partitioning within the rice panicle, Aust. J. Plant Physiol. 20 (1993) 231−241.

[3] J. Yang, C. Yunying, H. Zhang, L. Liu, J. Zhang, Involvement of polyamines in the post-anthesis development of inferior and superior spikelets in rice, Planta 228 (2008) 137−149.

[4] Z. Wang, Y. Xu, J. Wang, J. Yang, J. Zhang, Polyamine and ethylene interactions in grain filling of superior and inferior spikelets of rice, Plant Growth Regul. 66 (2012) 215−228.

[5] Y. Deng, Y. Yu, Y. Hu, L. Ma, Y. Lin, Y. Wu, Z. Wang, Z. Wang, J. Bai, Y. Ding, L. Chen, Auxin-mediated regulation of dorsal vascular cell development may be responsible for sucrose phloem unloading in large panicle rice, Front. Plant Sci. 12 (2021) 630997.

[6] C. You, H. Zhu, B. Xu, W. Huang, S. Wang, Y. Ding, Z. Liu, G. Li, L. Chen, C. Ding, S. Tang, Effect of removing superior spikelets on grain filling of inferior spikelets in rice, Front. Plant Sci. 7 (2016) 1161.

[7] Z. Zhang, J. Tang, T. Du, H. Zhao, Z. Li, Z. Li, W. Lin, Mechanism of developmental stagnancy of rice inferior spikelets at early grain-filling stage as revealed by proteomic analysis, Plant Mol. Biol. Rep. 33 (2015) 1844−1863.

[8] J. Fu, Y. Xu, L. Chen, L. Yuan, Z. Wang, J. Yang, Changes in enzyme activities involved in starch synthesis and hormone concentrations in superior and inferior spikelets and their association with grain filling of super rice, Rice Sci. 20 (2013) 120−128.

[9] G. Zhu, N. Ye, J. Yang, X. Peng, J. Zhang, Regulation of expression of starch synthesis genes by ethylene and ABA in relation to the development of rice inferior and superior spikelets, J. Exp. Bot. 62 (2011) 3907−3916.

[10] H. Zhang, H. Li, L. Yuan, Z. Wang, J. Yang, J. Zhang, Post-anthesis alternate wetting and moderate soil drying enhances activities of key enzymes in sucrose-to-starch conversion in inferior spikelets of rice, J. Exp. Bot. 63 (2012) 215−227.

[11] Z. Wang, Y. Xu, T. Chen, H. Zhang, J. Yang, J. Zhang, Abscisic acid and the key enzymes and genes in sucrose-to-starch conversion in rice spikelets in response to soil drying during grain filling, Planta 241 (2015) 1091−1107.

[12] N.M. Doll, G.C. Ingram, Embryo–endosperm interactions, Annu. Rev. Plant Biol. 73 (2022) 293−321.

[13] L. An, Y. Tao, H. Chen, M. He, F. Xiao, G. Li, Y. Ding, Z. Liu, Embryo-endosperm interaction and its agronomic relevance to rice quality, Front. Plant Sci. 11 (2020) 587641.

[14] J. Liu, M. Wu, C. Liu, Cereal endosperms: development and storage product accumulation, Annu. Rev. Plant Biol. 73 (2022) 255—291.

[15] Z. Lin, X. Zhang, X. Yang, G. Li, S. Tang, S. Wang, Y. Ding, Z. Liu, Proteomic analysis of proteins related to rice grain chalkiness using iTRAQ and a novel comparison system based on a notched-belly mutant with white-belly, BMC Plant Biol. 14 (2014) 163.

[16] Y. Tao, L. An, F. Xiao, G. Li, Y. Ding, M.J. Paul, Z. Liu, Integration of embryo–endosperm interaction into a holistic and dynamic picture of seed development using a rice mutant with notched-belly kernels, Crop J. 10 (2022) 729—742.

[17] Y. Chen, Y. Chen, C. Shi, Z. Huang, Y. Zhang, S. Li, Y. Li, J. Ye, C. Yu, Z. Li, X. Zhang, J. Wang, H. Yang, L. Fang, Q. Chen, SOAPnuke: a MapReduce acceleration-supported software for integrated quality control and preprocessing of high-throughput sequencing data, GigaScience 7 (2018) 1—6.

[18] A.M. Bolger, M. Lohse, B. Usadel, Trimmomatic: a flexible trimmer for Illumina sequence data, Bioinformatics 30 (2014) 2114—2120.

[19] D. Kim, B. Langmead, S.L. Salzberg, HISAT: a fast spliced aligner with low memory requirements, Nat. Methods 12 (2015) 357—360.

[20] B. Li, C.N. Dewey, RSEM: accurate transcript quantification from RNA-Seq data with or without a reference genome, BMC Bioinformatics 12 (2011) 323.

[21] L. Wang, Z. Feng, X. Wang, X. Wang, X. Zhang, DEGseq: an R package for identifying differentially expressed genes from RNA-seq data, Bioinformatics 26 (2010) 136—138.

[22] Z. An, Y. Zhao, H. Cheng, W. Li, H. Huang, Development and application of EST-SSR markers in Hevea brasiliensis Muell, Hereditas 31 (2009) 311—319 (in Chinese with English abstract).

[23] E. Howe, K. Holton, S. Nair, D. Schlauch, R. Sinha, J. Quackenbush, MeV: MultiExperiment Viewer, in: M.F. Ochs, J.T. Casagrande, R.V. Davuluri (Eds.), Biomedical Informatics for Cancer Research, Springer US, Boston, MA, 2010, pp. 267—277.

[24] M. Ashburner, C.A. Ball, J.A. Blake, D. Botstein, H. Butler, J.M. Cherry, A.P. Davis, K. Dolinski, S.S. Dwight, J.T. Eppig, M.A. Harris, D.P. Hill, L. Issel-Tarver, A. Kasarskis, S. Lewis, J.C. Matese, J.E. Richardson, M. Ringwald, G.M. Rubin, G. Sherlock, Gene Ontology: tool for the unification of biology, Nat. Genet. 25 (2000) 25—29.

[25] R.C. Team, R: a language and environment for statistical computing, R Foundation for Statistical Computing, Vienna, Austria, 2013.

[26] P. Chen, L. Chen, Z. Jiang, G. Wang, S. Wang, Y. Ding, Sucrose is involved in the regulation of iron deficiency responses in rice (*Oryza sativa* L.), Plant Cell Rep. 37 (2018) 789—798.

[27] H. Ning, J. Qiao, Z. Liu, Z. Lin, G. Li, Q. Wang, S. Wang, Y. Ding, Distribution of proteins and amino acids in milled and brown rice as affected by nitrogen fertilization and genotype, J. Cereal Sci. 52 (2010) 90—95.

[28] C. López-Cristoffanini, X. Serrat, O. Jáuregui, S. Nogués, M. López-Carbonell, Phytohormone profiling method for rice: effects of *GA20ox* mutation on the gibberellin content of japonica rice varieties, Front. Plant Sci. 10 (2019) 733.

[29] B.O. Juliano, A.P.P. Tuaño, Gross structure and composition of the rice grain, in: J. Bao (Ed.), Rice (Fourth Edition), AACC International Press, St. Paul, USA, 2019, pp. 31−53.

[30] H. Wei, Y. Zhu, S. Qiu, C. Han, L. Hu, D. Xu, N. Zhou, Z. Xing, Y. Hu, P. Cui, Q. Dai, H. Zhang, Combined effect of shading time and nitrogen level on grain filling and grain quality in japonica super rice, J. Integr. Agric. 17 (2018) 2405−2417.

[31] Z. Zhang, H. Zhao, F. Huang, J. Long, G. Song, W. Lin, The 14-3-3 protein GF14f negatively affects grain filling of inferior spikelets of rice (*Oryza sativa* L.), Plant J. 99 (2019) 344−358.

[32] J. Yang, S. Peng, Z. Zhang, Z. Wang, R.M. Visperas, Q. Zhu, Grain and dry matter yields and partitioning of assimilates in japonica/indica hybrid rice, Crop Sci. 42 (2002) 766−772.

[33] J. Yang, J. Zhang, Grain-filling problem in 'super' rice, J. Exp. Bot. 61 (2010) 1−5.

[34] M. Dong, J. Gu, L. Zhang, P. Chen, T. Liu, J. Deng, H. Lu, L. Han, B. Zhao, Comparative proteomics analysis of superior and inferior spikelets in hybrid rice during grain filling and response of inferior spikelets to drought stress using isobaric tags for relative and absolute quantification, J. Proteomics 109 (2014) 382−399.

[35] X. Zhang, J. Lei, D. Zheng, Z. Liu, G. Li, S. Wang, Y. Ding, Amino acid composition of leaf, grain and bracts of japonica rice (*Oryza Sativa* ssp. *japonica*) and its response to nitrogen fertilization, Plant Growth Regul. 82 (2017) 1−9.

[36] P.E. Jameson, J. Song, Cytokinin: a key driver of seed yield, J. Exp. Bot. 67 (2016) 593−606.

[37] X. Zhang, J. Tong, A. Bai, C. Liu, L. Xiao, H. Xue, Phytohormone dynamics in developing endosperm influence rice grain shape and quality, J. Integr. Plant Biol. 62 (2020) 1625−1637.

[38] T. Tang, H. Xie, Y. Wang, B. Lu, J. Liang, The effect of sucrose and abscisic acid interaction on sucrose synthase and its relationship to grain filling of rice (*Oryza sativa* L.), J. Exp. Bot. 60 (2009) 2641−2652.

[39] H. Zhang, G. Tan, L. Yang, J. Yang, J. Zhang, B. Zhao, Hormones in the grains and roots in relation to post-anthesis development of inferior and superior spikelets in japonica/indica hybrid rice, Plant Physiol. Biochem. 47 (2009) 195−204.

[40] C.C. Wu, P.K. Diggle, W.E. Friedman, Kin recognition within a seed and the effect of genetic relatedness of an endosperm to its compatriot embryo on maize seed development, Proc. Natl. Acad. Sci. U. S. A. 110 (2013) 2217−2222.

[41] G.C. Ingram, Family plot: the impact of the endosperm and other extra-embryonic seed tissues on angiosperm zygotic embryogenesis, F1000Res 9 (2020) 18.

[42] C.S.C. Cadman, P.E. Toorop, H.W.M. Hilhorst, W.E. Finch-Savage, Gene expression profiles of Arabidopsis Cvi seeds during dormancy cycling indicate a common underlying dormancy control mechanism, Plant J. 46 (2006) 805−822.

[43] T. Widiez, G.C. Ingram, J.F. Gutiérrez-Marcos, Embryo-endosperm-sporophyte interactions in maize seeds., in: B. Larkins (Ed.), Maize Kernel Development, 1st ed., CABI, UK, 2017, pp. 95−107.